Solid State Science and Technology, Vol. 26, No 1 (2018) 157-167
ISSN 0128-7389 | *http://journal.masshp.net*

CONDUCTING POLYMER BASED SENSOR EMBEDDED WITH BIMETALLIC Ni-Ag FOR DETECTION OF *E. Coli* IN WATER

Norshafadzila Mohammad Naim[1], Huda Abdullah[1],
Jamal Jurait[1] and Aidil Abdul Hamid[2]

[1]*Department of Electrical, Electronic and System Engineering,*
Faculty of Engineering and Built Environment,
Universiti Kebangsaan Malaysia, Malaysia.

[2]*School of Biosciences and Biotechnology, Faculty of Science and Technology,*
Universiti Kebangsaan Malaysia, Malaysia.

Corresponding author: shafadzilanaim@gmail.com

ABSTRACT

Conducting polymers can be suitable materials for microbe sensor because of the intrinsically conducting characteristic. Polyaniline (PANI) is found to be the most promising conducting polymer. The nanocomposite of PANI and bimetallic Ni-Ag was synthesized via sol-gel method. PANI-Ni-Ag thin films were deposited onto glass substrate using spin-coating technique. The films were characterized using XRD, AFM, TEM and UV-Vis spectroscopy. The performance of the sensor was conducted using *I-V* measurement to obtain the changes in the current before and after the exposure to *E. coli* bacteria in water. The peaks in XRD pattern confirmed the presence of Ni and Ag crystallite in face-centered cubic structures. AFM images indicate the increase of PANI-Ni-Ag surface roughness films while the concentration of Ni increased. TEM image shows the spherical silver and nickel nanoparticles. The resonance plasma band from UV-Vis spectroscopy is located at around 472 nm to 484 nm. *I–V* measurements show that the presence of *E. coli* has increased the current change of the films. From the sensitivity performance, the increase of Ag concentration in the samples has increased the sensitivity of the sensor.

Keywords: Polyaniline; Ag-Ni; thin films; E. coli sensor; sol-gel method

INTRODUCTION

Dissemination of harmful bacteria in food or water supplies as a result of accidents and pollution activity can produce serious consequences in the form of economic losses and human suffering. Gram-negative bacteria (e.g. *Escherichia coli* or *E. coli* O157:H7) are a leading cause of food-borne illnesses. It causes urinary tract infections, hemorrhagic colitis, inflammation, bloody diarrhea, peritonitis and occasionally hemolytic uremic syndrome (a type of kidney failure) [1]. The production of sensor which has high sensitivity and fast identification is important to prevent the infection of *E. coli*.

Conducting polymers are the new material and they are rapidly emerging by making the scientific and technological interest increasingly growing. This kind of polymers have already been found for extensive application in electrochemical biosensors, due to their electroactivitity, compatibility with biological molecules, environmental stability and ease of synthesis from inexpensive monomers [2,3]. Among the available intrinsically conducting polymers, polyaniline (PANI) is found to be the most promising because of its easy synthesis, low cost monomer, tunable properties, high conductivity, and better stability compared to others. Microbial detectors which are made from such organic polymer can help in identification of the microbes quickly and easily. For currently technology, polymeric sensors are the suitable ones for fabricating of microorganisms monitors [4- 6].

The conductivity of this conducting polymer can be controlled by the process of doping which may be carried out through a chemical, electrochemical or photochemical route [7]. The conductivity is characterized by charge transfer from dopant to polymer or from polymer to dopant [8]. The interaction between polyaniline and noble metals has attracted a great deal of interest in a wide variety of applications. The composite of polyaniline with metals have been widely used in many applications such as gas sensor [9,10], biosensor [11,12], fuel cell catalyst [13,14], electrochemical sensor [15], electrocatalyst [16], supercapasitor [17,18], etc. When metals ions are added into the synthesized system of polyaniline, the metal ions can interact with the nitrogen atoms in the polyaniline chains [19]. Silver and nickel has been proposed as alternate conductive filler in electrically conductive polymer composites for sensor applications, due to its high electrical conductivity, low electrical migration and high compatibility.

In this paper, we reported the synthesis of Ag-Ni doped polyaniline nanocomposite thin films to be applied as a biosensor to detect the presence of *E. coli* bacteria in water. *I-V* measurement was used in conducting the sensing performance by observing the change in current after incubated the sensor electrode into *E. coli*.

EXPERIMENTAL

Sample preparation

The metal precursor nickel nitrate ($Ni(NO_3)_2$) and silver nitrate ($AgNO_3$, 99.99% purity), the monomer aniline ($C_6H_5NH_2$), polyvinyl alcohol (PVA, 99% hydrolysis) were purchased from Sigma-Aldrich Chemicals. In this study, the nanocomposite of polyaniline (PANI) and metals were prepared by the oxidative polymerization of aniline and the reduction process of metal compound with the presence of nitric acid and PVA. 2.5 g PVA was dissolved in deionized water and stirred on the hot plate at 80^{o}C – 90^{o}C. Ag-Ni compound was synthesized by dissolving 0.5 g of nickel nitrate and silver nitrate in deionized water. The concentrations of Ni and Ag were varied using the formula of Ni_x-Ag_{1-x} with x represents the molar ratios of Ni and Ag (x = 0.8, 0.6, 0.4 and 0.2). When the PVA becomes completely dissolved, the solution transform into a

viscous transparent liquid, and then Ni-Ag solution was added drop by drop into PVA solution by using pipette. 1.25 mL of aniline was added to the solution followed by 1.0 M nitric acid (HNO_3). The mixture was stirred until the solution changed to a greenish dark brown liquid, indicate the solution become the PANI-Ni-Ag nanocomposite as shown in Figure 1. The nanocomposite solution was spin- coated onto glass substrate using photoresist spinner, with the speed of 2000 rpm for 15 s. The nanocomposite thin films were dried on the hot plate for 1 hour

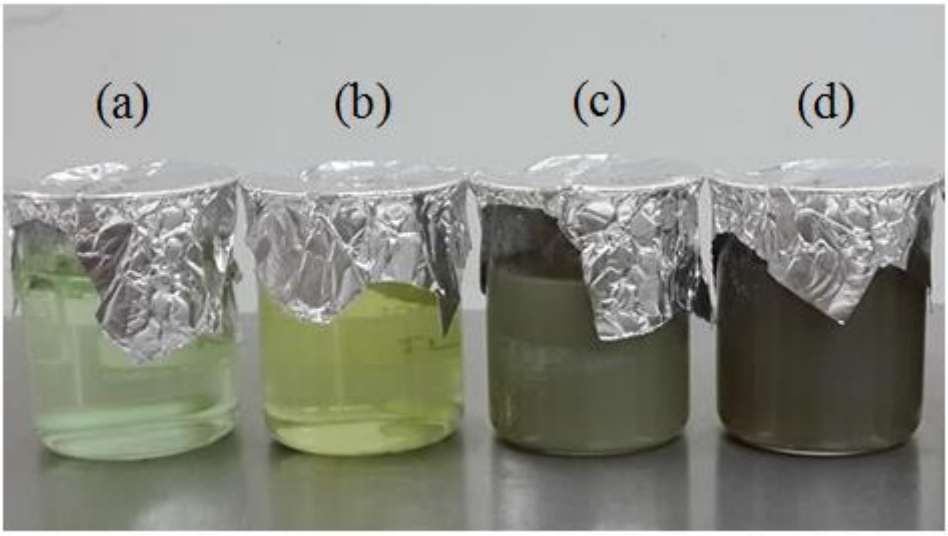

Figure 1: PANI-Ni_x-Ag_{1-x} nanocomposite solution; (a) PANI-$Ni_{0.8}$-$Ag_{0.2}$ (b) PANI-$Ni_{0.6}$-$Ag_{0.4}$ (c) PANI-$Ni_{0.4}$-$Ag_{0.6}$ (d) PANI-$Ni_{0.2}$-$Ag_{0.8}$.

Thin film characterization

X-ray diffraction analysis was conducted on Bruker model D8 Advanced X-ray diffractometer using CuK_α radiation (λ = 1.5406Å) and the measurement were performed in 2*q* range from 20º to 60º. Surface morphology of the thin films and the size of nanoparticles in PANI-Ni-Ag nanocomposite were studied from atomic force microscopy (AFM) and transmittance electron microscopy (TEM) respectively. The optical characterization of PANI- Ni-Ag thin films was carried out using Perkin Elmer UV-Visible spectroscopy. Sensor performance was conducted using GAMRY-Physical Electrochemistry.

Fabrication of sensor electrode

A comb-structure of silver electrode was sputtered on the nanocomposite thin film for 1000 Å thickness. Cu wires were soldered to the silver electrodes as the connection between thin film and the measuring device. The sensor electrode was connected to the power supply. Sensor was immersed into clean water and *E. coli* solution. *I-V* curve is obtained because electric flows on the film surface with the present of metals and conducting polymer.

RESULTS AND DISCUSSIONS

X-ray diffraction analysis

The X-ray diffraction patterns of PANI-Ni-Ag nanocomposite thin films were shown in Figure 2. The prominent peaks at 2*q* values of about 38.1° and 44.3° representing the (1 1 1) and (2 0 0) Bragg's reflections of face-centered cubic structure of silver while nickel share the same lattice plane at (2 0 0). The average crystallite sizes were calculated using Scherrer's equation [20]:

$$D = \frac{0.9\lambda}{\beta \cos\theta} \qquad (1)$$

where λ=0.154 nm is the wavelength of X-ray for CuKα, β is FWHM (full width at half maximum intensity of the peak), q is the diffraction angle and D is the crystallite size. The values of the calculated crystallite size have been summarized in Table 1.

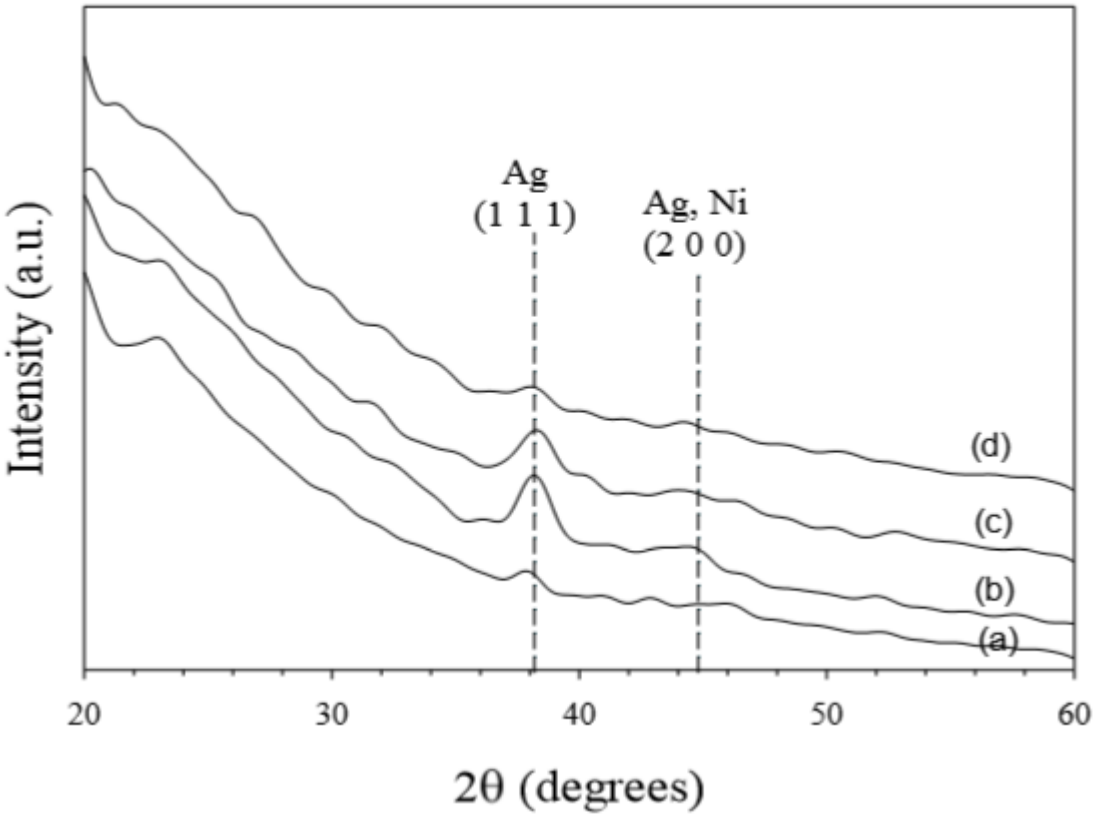

Figure 2 XRD spectra of PANI-Ni_x-Ag_{1-x} nanocomposite thin films; (a) PANI-$Ni_{0.8}$-$Ag_{0.2}$ (b) PANI- $Ni_{0.6}$-$Ag_{0.4}$ (c) PANI-$Ni_{0.4}$-$Ag_{0.6}$ (d) PANI-$Ni_{0.2}$-$Ag_{0.8}$

Table 1: Calculated crystallite size of PANI-Ni-Ag nanocomposite thin films

Molar ratio		Crystallite size (nm)
Ni	**Ag**	
0.8	0.2	13.17
0.6	0.4	11.79
0.4	0.6	11.02
0.2	0.8	10.67

Atomic force microscopy (AFM).

AFM was used to examine the morphology of the surface of PANI-Ni-Ag nanocomposite thin films. To evaluate the surface roughness as well as the grain size of the films, an area of 1µm x 1µm was scanned in tapping mode. Figure 3 shows the morphology of PANI-Ni-Ag nanocomposite thin films surface with different concentration of Ni-Ag. The average surface roughness and grain size were being listed in Table 2. As the Ag concentration decreased and Ni concentration increased, both surface roughnesses and grain sizes are found to be increased. The addition of Ag concentration in PANI-Ni-Ag nanocomposite causes the well-dispersion of the particles and changes the film surface become smoother. The reduction of average roughness and grain size data was in parallel with the reduction of the crystallite size in XRD data.

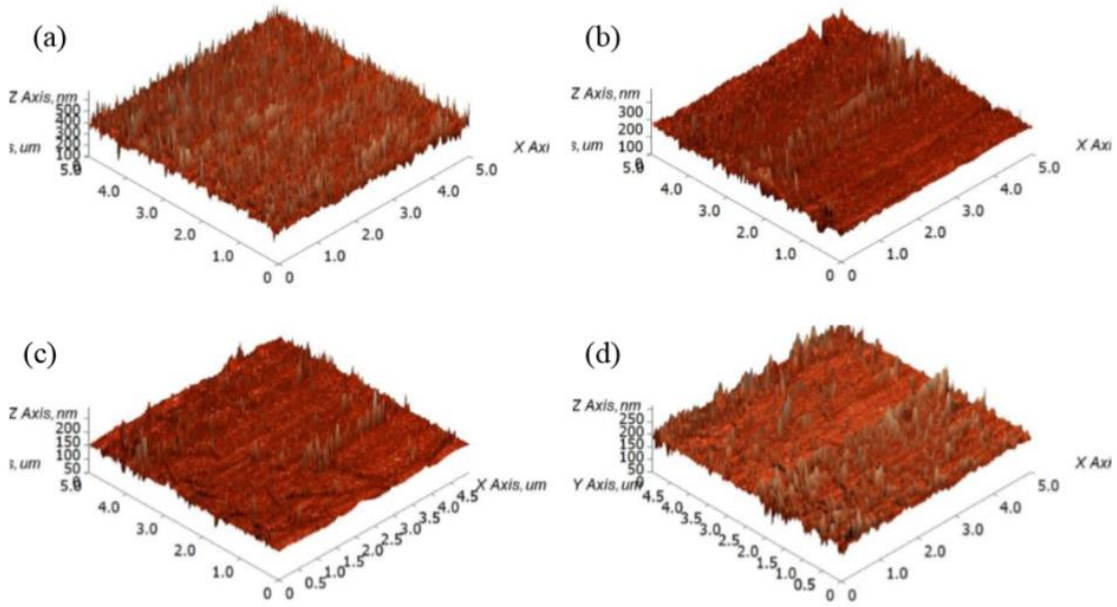

Figure 3: AFM images of PANI-Ni_x-Ag_{1-x} nanocomposite thin films; (a) PANI-$Ni_{0.8}$-$Ag_{0.2}$ (b) PANI- $Ni_{0.6}$-$Ag_{0.4}$ (c) PANI-$Ni_{0.4}$-$Ag_{0.6}$ (d) PANI-$Ni_{0.2}$-$Ag_{0.8}$.

Table 2: Average roughness and grain size of PANI-Ag-Ni nanocomposite thin films

Molar ratio		Average roughness (nm)	Grain size (nm)
Ni	**Ag**		
0.8	0.2	22.20	77.0
0.6	0.4	16.96	40.9
0.4	0.6	11.03	18.6
0.2	0.8	8.98	19.9

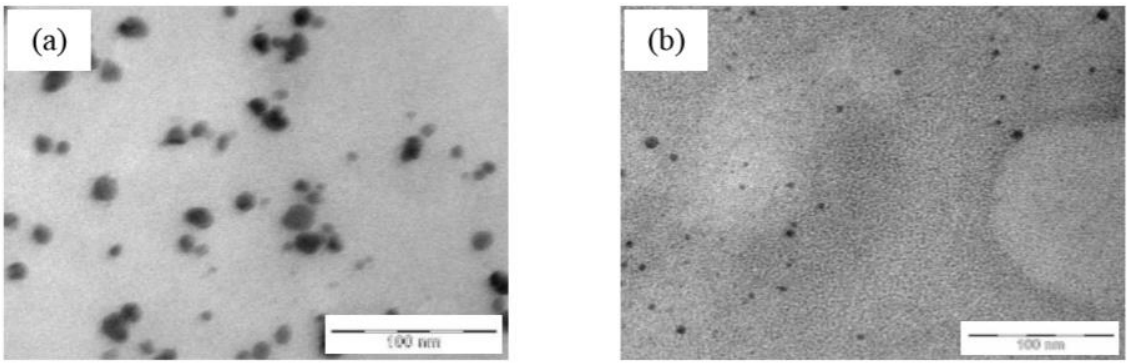

Figure 4: TEM images of (a) PANI-$Ni_{0.8}$-$Ag_{0.2}$ and (b) PANI-$Ni_{0.2}$-$Ag_{0.8}$ nanocomposite thin films

Transmittance electron microscopy (TEM).
TEM microphotograph shows the comparison of PANI-$Ni_{0.8}$-$Ag_{0.2}$ nanocomposite in Figure 4 (a) and PANI-$Ni_{0.2}$-$Ag_{0.8}$ nanocomposite in Figure 4 (b). As we can see in the TEM images, the particles in Figure 4 (a) are larger than that in Figure 4 (b). Figure 4 (a) contains more the nanoparticles of Ni than Ag which are in spherical shape and diameter size range from ~5 nm to ~30 nm. Figure 4 (b) contains well-dispersed of more Ag nanoparticles than Ni particles which are in spherical shape and diameter size range from ~5 nm to ~10 nm. The existence of Ni nanospherical in PANI matrix also has been reported by Liu et al. (2010) [21]. Incorporation of more Ni particles than Ag particles with the presence of PANI makes the particle size larger and some of them agglomerated as we can see in Figure 4 (b).

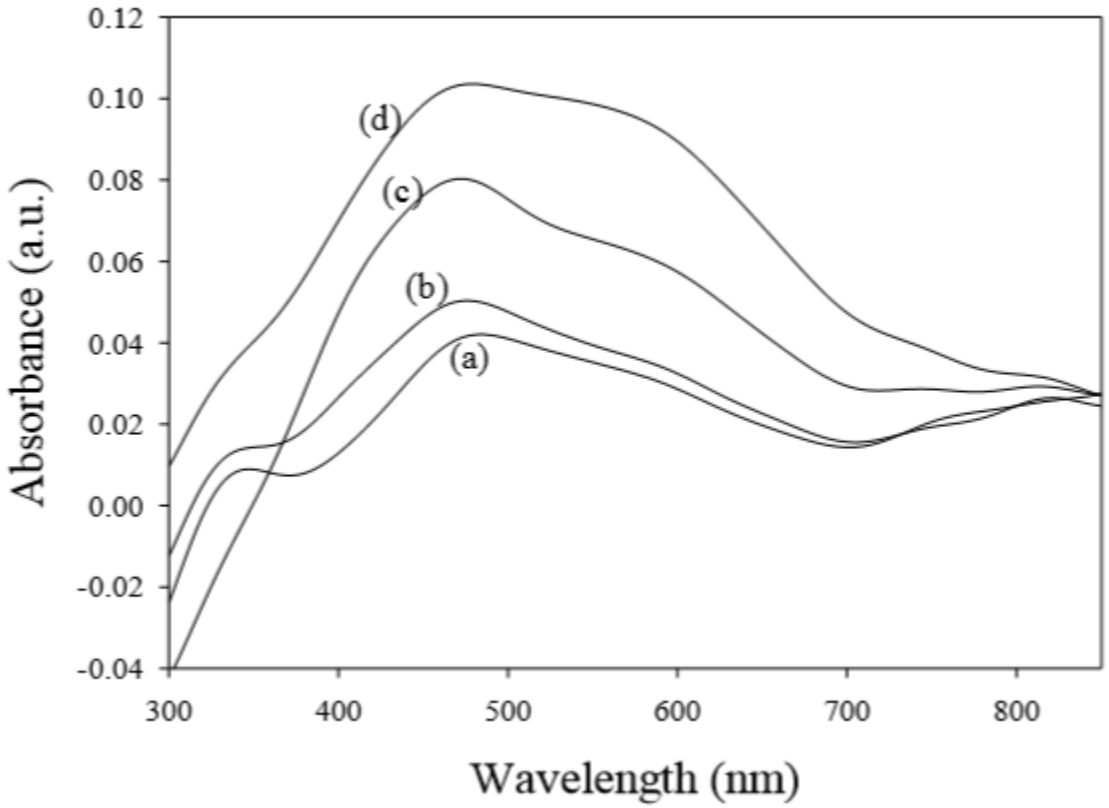

Figure 5: UV-Vis absorption spectra of PANI -Ni_x-Ag_{1-x} nanocomposite thin films; (a) PANI-$Ni_{0.8}$- $Ag_{0.2}$ (b) PANI-$Ni_{0.6}$-$Ag_{0.4}$ (c) PANI-$Ni_{0.4}$-$Ag_{0.6}$ (d) PANI-$Ni_{0.2}$-$Ag_{0.8}$.

UV-Vis spectroscopy

UV-Vis absorption is performed to verify the presence of silver and nickel nanoparticles in the prepared samples of PANI-Ni-Ag nanocomposite thin films as shown in Figure 5. The spectra contain maximum absorption band at 484 nm, 475 nm, 472 nm and 479 nm in Figure 5(a), 6(b), 6(c) and 6(d) respectively. The addition of Ag concentration into PANI-Ni-Ag nanocomposite with the decrease of Ni content results the significantly increase in absorbance. This trend is corresponding to the analysis studied by Lee et al. (2009) which also reported absorption spectra of Ag-Ni alloy nanoparticles with various Ag/Ni molar ratios [22]. According to Mie theoretic calculations, the absorption spectrum for Ni has a very weak peak around 330 nm [23]. Most literature reports show no absorption band for Ni nanoparticles, but the presence of Ni can dampen the Ag plasmon band and shift it red.

Sensor performance

The performance of the prototype biosensor has been measured through the *I-V* measurement to study the current change of the thin film sensor with and without incubation to *E. coli*. The concentrations of *E. coli* in the solution were fixed to 3.57 x 10^8 CFU/mL for each testing. Figure 6 describes the change of current for PANI-Ni-Ag nanocomposite thin films when the sensor films were immersed in deionized water and

E. coli solution. The results show PANI-$Ni_{0.2}$- $Ag_{0.8}$ nanocomposite performed the higher sensitivity among the other samples. The current is apparently changed when the sensor film was immersed in *E. coli* solution. This proves the existence of interactions between metal and microbe. When the sensor films are immersed into *E. coli* solution, the metal ions and metal nanoparticles on the PANI-Ni-Ag thin film surface interact with the microbe. The positive charged of Ag^+ and Ni^+ could be attached to the negatively charged *E. coli* [24]. The metabolism of the microbe creates an acid environment for the release of metal ions and it is believed that the silver ions interact with bacterial cell walls, plasma membranes, bacterial DNA and proteins, as well as ribosomes, resulting in bactericidal effects [5]. The metal and microbe interactions are mainly related to the cell wall and outer membrane arrangement. This is due to the significant differences in the outer layers of Gram-negative and Gram-positive bacteria. The cell wall of gram-negative bacteria consists of lipids, protein and lipopolysaccharides (LPS) that ensure more effective defense against biocides in comparison to gram positive bacteria where the cell wall does not contains outer membrane of LPS [25]. Since *E. coli* are gram-negative bacteria, they possess an outer membrane and unique periplamic spaces [26], thus *E. coli* are more susceptible to silver nanoparticles.

The sensitivity (*S*) of a sensor is described as the ratio of the magnitude of response upon exposure to the microbe (I_e) to that of without exposure to the microbe (I_o). Figure 7 shows the graph of sensitivity (*S*) on *E. coli* against the annealing temperature of PANI-Ni-Ag nanocomposite thin films which is calculated using the formula [27]:

$$S = \frac{(I_e - I_o)}{I_o} \times 100 \qquad (2)$$

where *S* is the sensitivity of sensor electrode on *E. coli*, I_e is the current when the sensor electrode exposure to *E. coli* and I_o is the current when the sensor electrode not exposure to *E. coli*. The graph shows as the Ag concentration increased, the sensitivity of PANI-Ni-Ag nanocomposite thin film sensor become higher.

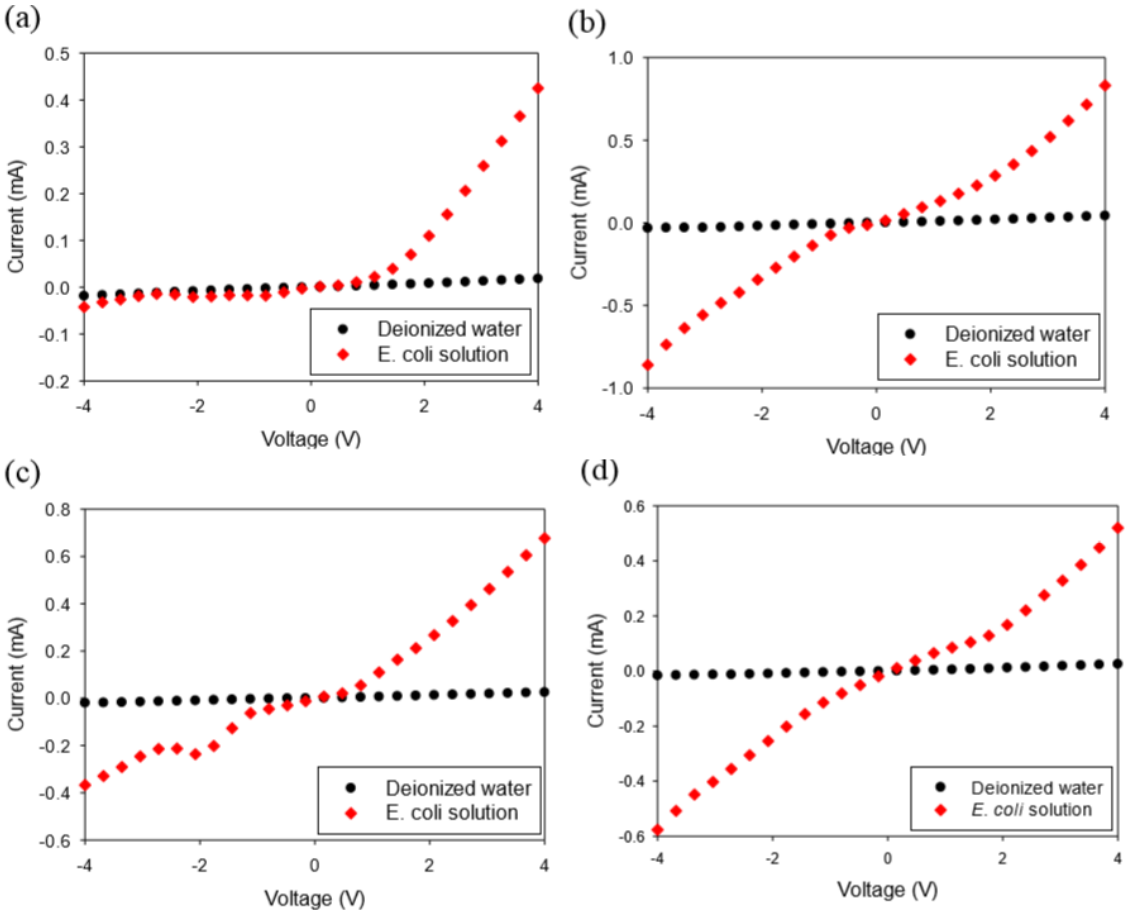

Figure 6: *I-V* measurements of PANI-Ni_x-Ag_{1-x} nanocomposite thin films; (a) PANI-$Ni_{0.8}$-$Ag_{0.2}$ (b) PANI-$Ni_{0.6}$-$Ag_{0.4}$ (c) PANI-$Ni_{0.4}$-$Ag_{0.6}$ (d) PANI-$Ni_{0.2}$-$Ag_{0.8}$, when the films were incubated in deionized water and *E. coli* solution

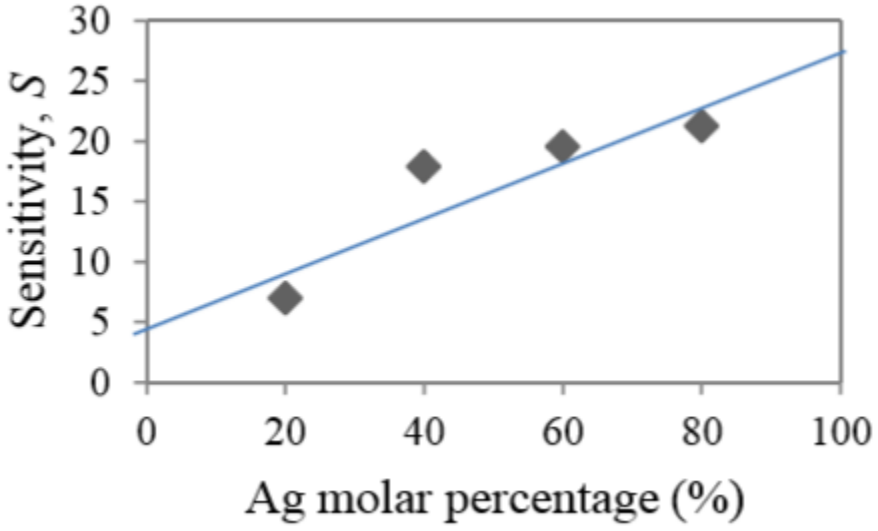

Figure 7: Sensitivity (*S*) on *E. coli* for PANI-Ni-Ag nanocomposite thin films with different molar ratio of Ag (%)

CONCLUSION

In conclusion, PANI-Ni-Ag nanocomposite thin films were synthesized by sol-gel method with chemical oxidative polymerization of aniline monomer to be applied as *E. coli* contamination sensor. Ni-Ag concentrations are varied to find the optimum concentration to detect microorganisms. The performance of sensor has been conducted using *I-V* measurement in deionized water and *E. coli* solution. The change in current when the sensor electrode incubated in *E. coli* proves the existence of interactions between metal and microbe. The result shows PANI- $Ni_{0.2}$-$Ag_{0.8}$ nanocomposite thin film performed the higher sensitivity among the other samples. It indicates that the presence of Ag nanoparticles gives more influence than Ni to develop the sensitivity of the sensor electrode on *E. coli*.

ACKNOWLEDGEMENTS

This project was supported by Exploratory Research Grants Scheme (ERGS/1/2012/STG05/ UKM/02/5), Islamic Educational, Scientific and Cultural Organization (ISESCO) (KK-2013-006), and Photonic Technology Laboratory, Department of Electrical, Electronic and System Engineering, University Kebangsaan Malaysia, Bangi, Selangor, Malaysia.

REFERENCES

[1] G.R. Kravitz, K. Smith, L. Wagstrom, *Clin. Infect. Dis.* **35** 103–105 (2002)
[2] E.B.Setterington, E.C. Alocilja, *Biosens. Bioelectron.* **26** 2208–2214 (2011)
[3] T. Ahuja, I. Ahmad Mir, D. Kumar, Rajesh, *Biomaterials* **28** 791–805 (2007)
[4] N.A. Noor Azmy, H. Abdullah, N. Mohammad Naim, A. Abdul Hamid, S. Shaari, W.H.M. Wan Mokhtar, *Radiat. Phys. Chem.* **103** 108–113 (2014)
[5] L. Guo, W. Yuan, Z. Lu, C.M. Li, *Colloid. Surface. A* **439** 69–83 (2013)
[6] R. Singh, R. Verma, G. Sumana, A.K. Srivastava, S. Sood, R.K. Gupta, B.D. Malhotra, *Bioelectrochemistry* **86** 30–37 (2012)
[7] S.M. Reda, S.M. Al-Ghannam, *Adv. Mater. Phys. Chem.* **2** 75–81 (2012)
[8] Shumaila, G.B.V.S. Lakshmi, M. Alam, A. M. Siddiqui, M. Zulfequar, M. Husain, *Curr. Appl. Phys.* **11** 217–222 (2011)
[9] S.C.K. Misra, P. Mathur, B.K. Srivastava, *Sensor. Actuat. A* **114** 30–35 (2004)
[10] A. Choudhury, *Sensor. Actuat. B* **138** 318–325 (2009)
[11] X. Feng, R. Li, Y. Ma, Q. Fan, W. Huang, *Synthetic Met.* **161** 1940–1945 (2011)
[12] X. Chen, Z. Chen, J. Zhu, C. Xu, W. Yan, C. Yao, *Bioelectrochemistry* **82** 87–94 (2011)
[13] B. Lai, P. Wang, H. Li, Z. Du, L. Wang, S. Bi, *Bioresource Technol.* **131** 321–324 (2013)
[14] Z. Mo, H. Peng, H. Liang, S. Liao, *Electrochim. Acta* **99** 30–37 (2013)
[15] K.J. Huang, J.Z. Zhang, Y.J. Liu, L.L. Wang, *Sensor. Actuat. B* **194** 303–310

(2014)
[16] Z.S. Yin, T.H. Hu. J.L. Wang, C. Wang, Z.X. Liu, J.W. Guo, *Electrochim. Acta.* **119** 144–154 (2014)
[17] H. Xu, J. Li, Z. Peng, J. Zhuang, J. Zhang, *Electrochim. Acta* **90** 393–399 (2013)
[18] S. Giri, D. Ghosh, C. K. Das. *J. Electroanal. Chem.* **697** 32–45 (2013)
[19] Y. Tan, Y. Zhang, J. Kan, *Express. Polym. Lett.* **3** (6) 333–339 (2009)
[20] I. Saini, J. Rozra, N. Chandak, S. Aggarwal, P.K. Sharma, A. Sharma, *Mater. Chem. Phys.* **139** (2–3) 802-810 (2013)
[21] R. Liu, H. Qiu, H. Li, H. Zong, C. Fang, *Synthetic. Met.* **160** 2404–2408 (2010)
[22] C.C. Lee, Y.Y. Cheng, H.Y. Chang, D.H. Chen, *J. Alloy Compd* **480** 674–680 (2009)
[23] Z. Zhang, T.M. Nenoff, J.Y. Huang, D.T. Berry, P.P. Provencio, *J. Phys. Chem. C* **113** 1155–1159 (2009)
[24] H. Su, Q. Ma, K. Shang, T. Liu, H. Yin, S. Ai, *Sensor. Actuat. B* **161** 298–303 (2012)
[25] R. Bryaskova, D. Pencheva, G. M. Kale, U. Lad, T. Kantardjiev, *J. Colloid Interf. Sci.* **349** 77– 85 (2010)
[26] J. Díaz-Visurraga, C. Gutiérrez, C. von Plessing, A. García, Metal nanostructures as antibacterial agents, Science against Microbial Pathogens: Communicating Current Research and Technological Advances, Formatex (2011) 210–218
[27] Kim. J. S. *J. Ind. Eng. Chem.*, **13** (4) 566–570 (2007)